

Research Paper

Comparative Analysis of Acoustic Emission Signals from On-Load Tap-Changers for Potential Detecting of Non-Simultaneous OperationsAndrzej CICHON¹, Sebastian BORUCKI, Michał WŁODARZ*

*Department of Electric Power Engineering and Renewable Energy
Faculty of Electrical Engineering, Automatic Control and Informatics
Opole University of Technology
Opole, Poland*

Corresponding Author e-mail: michal.wlodarz@student.po.edu.pl(received May 18, 2023; accepted January 21, 2024; published online March 19, 2024)*

The research reported in this paper deals with the potential of detecting non-simultaneous operation in on-load tap-changer (OLTC) using an acoustic emission method. Tests conducted under laboratory conditions were carried out using an OLTC model. Three transducers with different characteristics were used: WD 17 AH, D9241A, and R15 α , alongside oscillography as the reference method. The use of two new descriptors in the time domain was proposed. The feasibility of detecting the defect with different piezoelectric transducers was investigated.

As a result of the analysis of the results, it was found that each piezoelectric transducer can identify non-simultaneous operation of the switch. The most significant changes in descriptor values occurred in the time domain, and the most effective transducer turned out to be R15 α .

Keywords: acoustic emission; on-load tap-changer; piezoelectric transducer.



Copyright © 2024 The Author(s).
This work is licensed under the Creative Commons Attribution 4.0 International CC BY 4.0
(<https://creativecommons.org/licenses/by/4.0/>).

1. Introduction

Maintaining the appropriate quality parameters of transmission networks constitutes an important task for electricity distributors. One of the critical parameters is the voltage level, which affects how reactive power flows through the network. Voltage levels in an electric power system can fluctuate for various reasons, including changes in energy demand. The on-load tap-changer (OLTC) enables to adjust the voltage levels in power lines by changing the transformer's turn ratio. This is achieved by changing the number of active turns in the secondary winding. The OLTC switching mechanism is designed to work while the transformer is in use, without the need to shut the unit down.

Power transformers, crucial components of the transmission network, significantly impact the stability of power system operation. Although these devices have a relatively low failure rate, the potential cost to power utilities is very high in the event of an incident.

The OLTC is a component of transformers and it has the highest failure rate, making its diagnosis an important issue (MAJCHRZAK *et al.*, 2016). The causes of OLTC damage can be divided into three groups (JONGEN *et al.*, 2014):

- failure of the mechanical system, mainly related to the torque transmission system;
- damage to the main circuit, due to wear or damage to the contacts;
- damage to the insulation system.

During OLTC operation, the mechanical energy generated by the drive is stored in a mechanical energy accumulator in the form of two parallel springs. If one spring breaks, the switching process is extended, which can lead to resistor overheating (DUAN, WANG, 2015).

The contacts of the switch are affected by degradation due to arcing. Excessive contact wear can lead to an increase in contact resistance, which raises the temperature of these components and accelerates their

degradation (KANG, BIRTHWHISTLE, 2001a; 2001b; SCHELLHASE *et al.*, 2002). If their contact degradation varies between phases, asymmetrical contact switching may occur.

The oscillographic method has been established and widely used for assessing the condition of OLTCs. It uses the characteristic changes in the current flowing through the OLTC during switching to determine the degree of wear in current path components and the mechanical system (BORICIC *et al.*, 2019; JONGEN *et al.*, 2012). Dynamic resistance measurement takes a similar course to the oscillographic method. The main difference is that the resistance between the OLTC terminals is measured during switching instead of the current (AZIZ *et al.*, 2014; OSMANBASIC, SKELO, 2017). A disadvantage of these methods is that the unit must be taken out of service. Due to the strategic importance of transformers in electricity grids, shutting them down for diagnostic purposes is problematic and it is associated with additional costs for energy distributors.

Acoustic signals are generated during the OLTC switching process. Their source may be associated with the switch's mechanical system, contacts operation, or electrical discharges. The switches are mounted in containers filled with oil, and the acoustic waves generated are transmitted to the metal walls of the tank. This makes it possible to record acoustic emission (AE) signals using piezoelectric transducers. The recorded AE signals provide information characterizing the operation of the OLTC, enabling the diagnosis of the device using these signals (CICHOŃ *et al.*, 2011a; 2011b; LI *et al.*, 2012).

The most important advantage of the AE method is that diagnostic tests can be carried out online, eliminating the need to shut down the transformer. In addition, the AE method can be used simultaneously to determine the mechanical condition of the switch and to detect partial discharges (CICHOŃ *et al.*, 2011b; 2012; SECIC, KUZLE, 2017; SEO *et al.*, 2017). However, acoustic interference generated by the transformer and surrounding devices can lead to a reduction in the effectiveness of this diagnostic method. Besides, the time waveforms of the AE signals generated during power switch operation are difficult to interpret. A correct diagnosis requires expert knowledge, so artificial intelligence (AI) tools are proposed (WOTZKA, CICHOŃ, 2020; WOTZKA *et al.*, 2019).

This article, which constitutes a follow-up of research conducted for several years at Opole University of Technology, presents the results of measurements using the oscillographic and AE methods. Tests were carried out on two systems: one without defects and another where non-simultaneous operation occurred. The main goal of the research was to determine the possibility of detecting non-simultaneous operation of the OLTC using piezoelectric transducers with different transmission characteristics. In addition, a compar-

ative analysis of the used transducers was performed to determine the most effective means of detecting the asymmetry in system operation. A proposal for two new descriptors describing AE signals in the time domain is presented. The article presents the differences in these descriptors between the normal system and the modelled defect. Also, methods for determining descriptors based on the transducer used are proposed.

2. Experimental setup

The research focused on the analysis of the OLTC's operating stage when changes occurred in the selector tap position under the control of the power switch. Tests were conducted in a laboratory setting using an OLTC model with a separate selector and a VEL-110 power switch. An actual OLTC system with a selector shortened to six taps was used to create the test bench. The switch, together with the selector, was placed in a tank filled with insulating oil. There were pin-outs on the top cover of the tank to allow testing OLTC with the current flow. The measuring system was equipped with a motor that allowed switching. Three single-phase transformers were used to simulate the impedance of the transformer windings. The setup utilized in this study provides a range of defects that can be modeled: contact wear, non-simultaneous switching, and spring failure. A PLC was also installed to automate switching operations, thus speeding up measurements.

The non-simultaneous operation of the OLTC was simulated by changing contacts from new to worn ones. The degree of wear was simulated by milling the appropriate thickness of the original contact. The changes in the contact thickness used during research were as follows:

- phase A – 2 mm;
- phase B – 3 mm;
- phase C – 0 mm.

During oscillographic measurements, DC flows through the OLTC. During switching, there occur changes in the value of the current. The degree of wear of the device can be determined based on waveform. The results obtained with this method were used as a reference for the AE method during the tests.

MT-3, an instrument measuring basic transformer parameters, was used for oscillographic measurements. It can measure the dynamic change in current passing through OLTC during switching. MT-3 samples the current signal at a frequency of 8120 Hz. The manufacturer of the MT-3 also provides OLTC.exe software to assist diagnosticians in assessing the condition of the transformer or OLTC (Energo-Complex, 2008).

During switching, the OLTC generates sounds that are transmitted to the metal tank due to the presence of insulating oil. The AE waveforms carry information

about the switching process. The main goal of the research was to determine the feasibility of using these data for the OLTC diagnosis.

Laboratory tests were carried out using an OLTC model. Transducers with different characteristics were used to determine the diagnostic capability of OLTC in various frequency bands. The summary of their technical data is presented in Table 1. The transducers are referred to as 1, 2, and 3. The possibility of using different transducers for AE diagnostics will be evaluated during the study.

Table 1. Technical data of the transducers used (MISTRAS Group, n.d.a; n.d.b; n.d.c).

| No. | Type | Frequency band [kHz] | Peak sensitivity, Ref V/[m/s] | Peak sensitivity, Ref V/ μ bar |
|-----|--------------|----------------------|-------------------------------|------------------------------------|
| 1. | WD 17 AH | 100–900 | 56 dB | –61 dB |
| 2. | D9241A | 20–60 | 82 dB | – |
| 3. | R15 α | 50–400 | 80 dB | –63 dB |

All transducers were mounted by means of magnetic holders. They were connected to amplifiers via pre-amplifiers. The gains of both components are presented in Table 2.

Table 2. Preamplifiers and amplifiers gains.

| No. | Preamplifier gain [dB] | Amplifier gain [dB] |
|-----|------------------------|---------------------|
| 1. | 20 | 15 |
| 2. | 20 | 3 |
| 3. | 20 | 9 |

For recording AE waveforms, the Acquittek CH3160 measuring card was used, operating at a sampling frequency of 350 kHz. It was coupled with a laptop with the installed AcquiFlex software. Figure 1 depicts the measurement procedure.

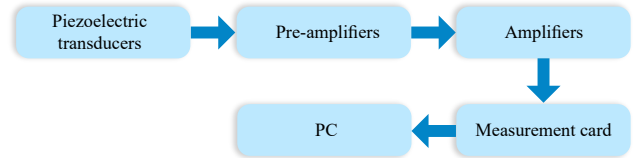


Fig. 1. Measurement procedure.

3. Results

The oscillographic method was used to verify whether an asymmetry of operation occurred in the system following its modification. The results obtained with the AE method will be compared to this method. The results obtained for normal system performance are presented in Fig. 2 and the results for the system with the modeled non-simultaneous operation are shown in Fig. 3.

Characteristic points of the waveforms corresponding to individual switching stages are marked with red lines. For the normal system, it can be observed that for each phase, the switching steps coincide in time, while for the modified system, they occur at different moments. Based on the results obtained, it can be concluded that, after the modification, there is a non-simultaneous operation in the system. A summary of the characteristic times and the differences between each phase is given in Table 3.

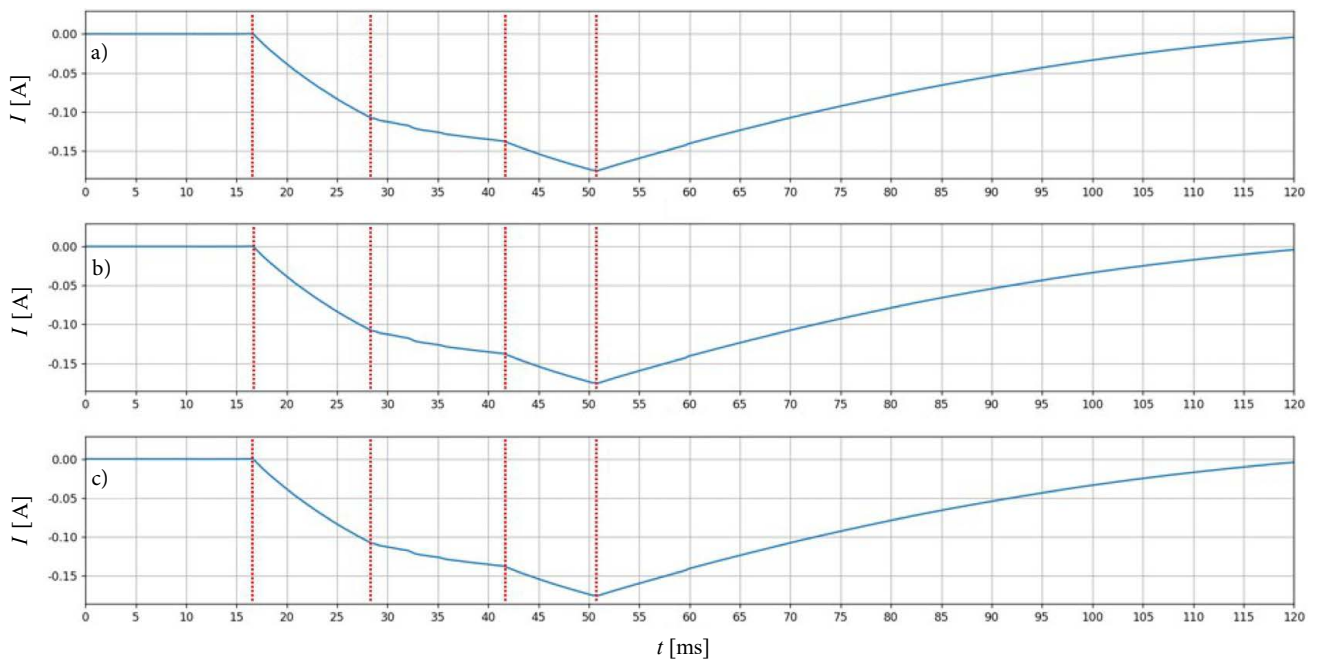


Fig. 2. Oscillographic waveforms for a symmetric system: a) phase A; b) phase B; c) phase C.

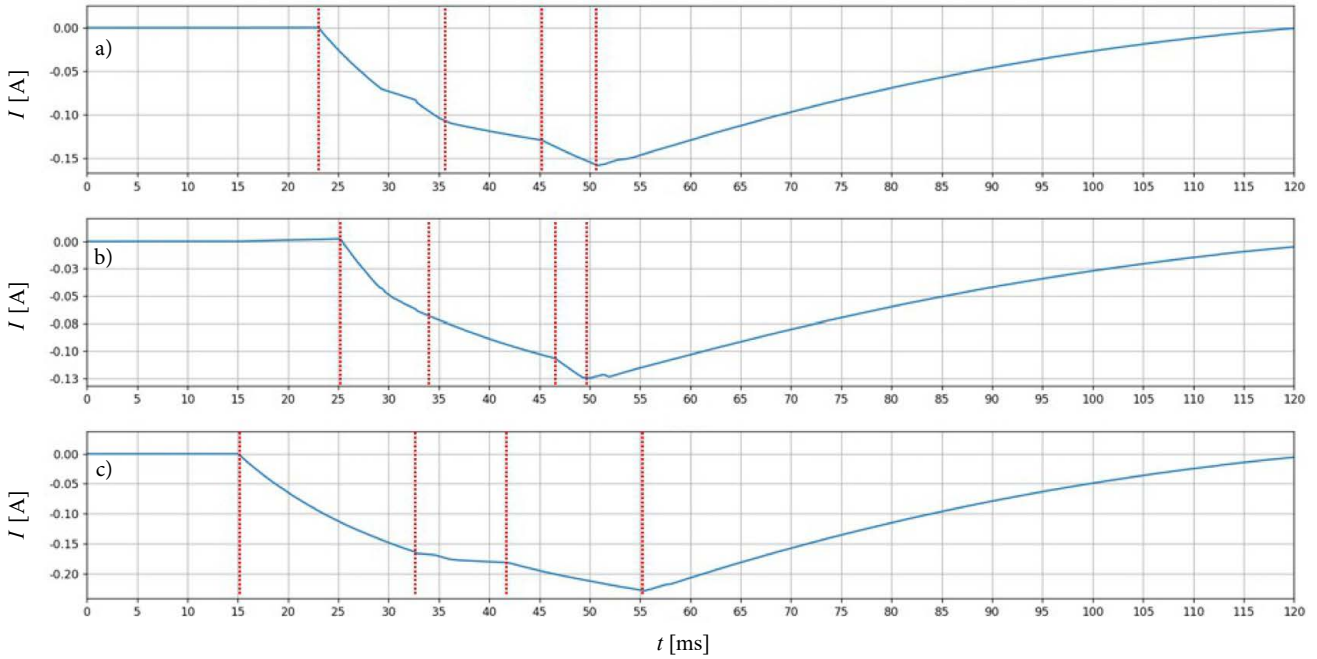


Fig. 3. Oscillographic waveforms for an asymmetric system: a) phase A; b) phase B; c) phase C.

Table 3. Characteristic times read and time differences between the phases.

| Simultaneous operation | | | | | |
|----------------------------|-------|-------|----------------------|-------|------|
| Characteristic times [ms] | | | Time difference [ms] | | |
| A | B | C | A–B | B–C | C–A |
| 16.90 | 16.80 | 16.90 | 0.10 | 0.10 | 0.00 |
| 28.90 | 28.90 | 29.10 | 0.00 | 0.20 | 0.20 |
| 41.50 | 41.40 | 41.50 | 0.10 | 0.10 | 0.00 |
| 50.70 | 50.70 | 50.80 | 0.00 | 0.10 | 0.10 |
| Non-simultaneous operation | | | | | |
| Characteristic times [ms] | | | Time difference [ms] | | |
| A | B | C | A–B | B–C | C–A |
| 23.10 | 25.00 | 15.00 | 1.90 | 10.00 | 8.10 |
| 36.00 | 37.40 | 32.80 | 1.40 | 4.60 | 3.20 |
| 45.20 | 46.60 | 41.90 | 1.40 | 4.70 | 3.30 |
| 50.70 | 49.60 | 55.40 | 1.10 | 5.80 | 4.70 |

Subsequently, the waveforms for the standard system and the modified one were juxtaposed to determine the possibility of diagnosing the modeled fault using the AE method. All signals were normalized by dividing by the maximum value. No filter was used during signal analysis. The results for each of the three transducers are given in Figs. 4–6.

A clear difference can be observed between the symmetrical and asymmetrical systems. The interval describing contact switching is between 40 and 90 ms. In this interval, significantly more acoustic events with smaller amplitudes can be observed for the system with non-simultaneous operation compared to the case of the normal system. This is due to the non-

simultaneous contact closure between the phases. For the normal system, these events occur simultaneously for each phase.

For the accurate determination of the technical feasibility of individual transducers, two descriptors were determined. Firstly, the envelope of the AE signal was determined and then the time at which the envelope is above the threshold of 0.05 was determined. The envelope was obtained by determining the local maxima for which polynomial interpolation was used. The threshold was adjusted by analyzing several time courses and conducting simulations for different values. An example of the determination process is shown in Fig. 7. In this way, the duration of the switching operation was

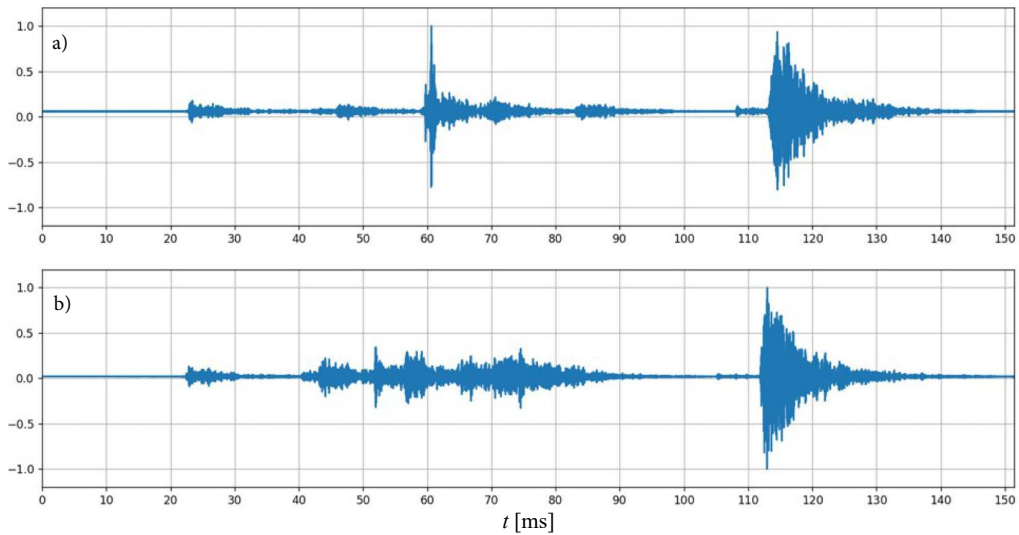


Fig. 4. AE signal generated by OLTC recorded with transducer 1 for:
a) system without asymmetry; b) system with asymmetry.

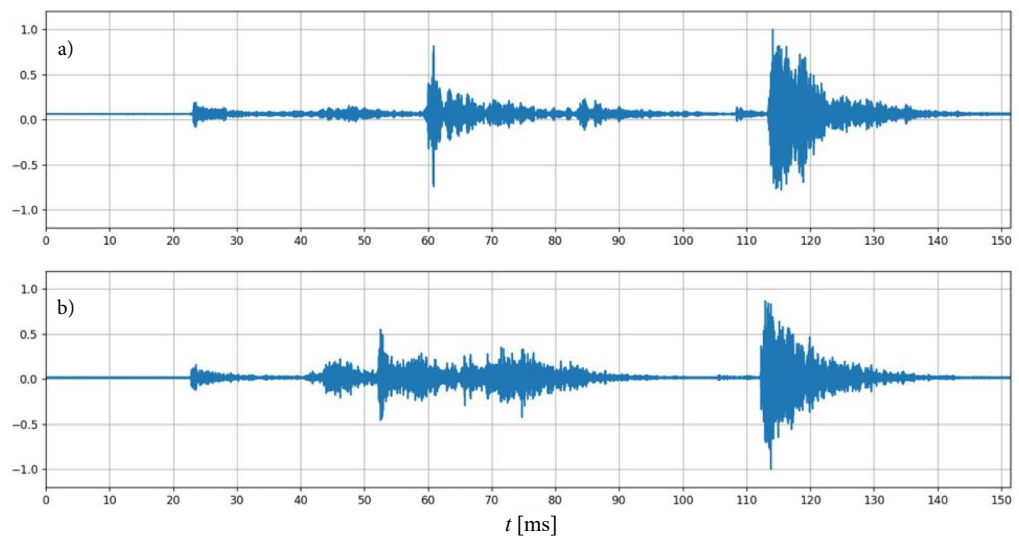


Fig. 5. AE signal generated by OLTC recorded with transducer 2 for:
a) system without asymmetry; b) system with asymmetry.

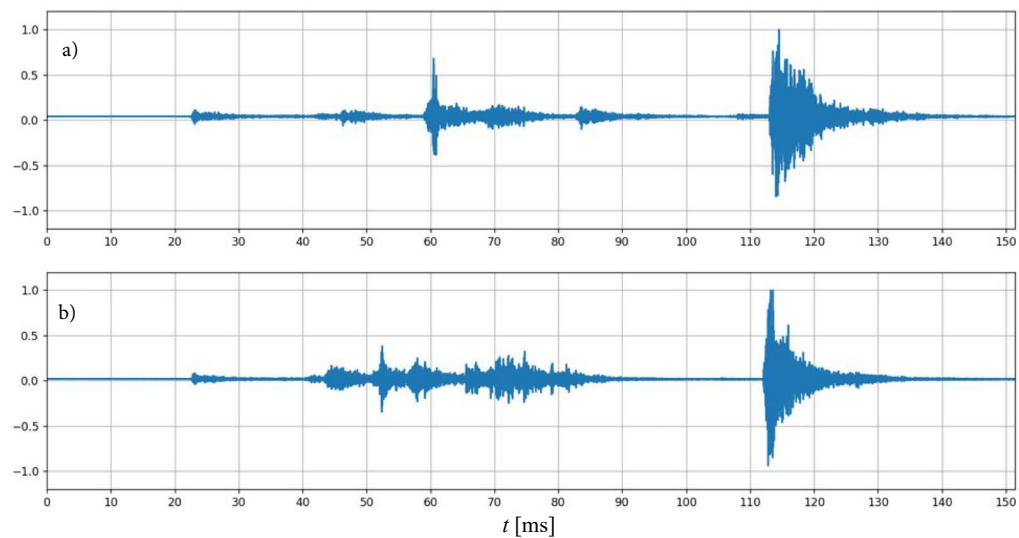


Fig. 6. AE signal generated by OLTC recorded with transducer 3 for:
a) system without asymmetry; b) system with asymmetry.

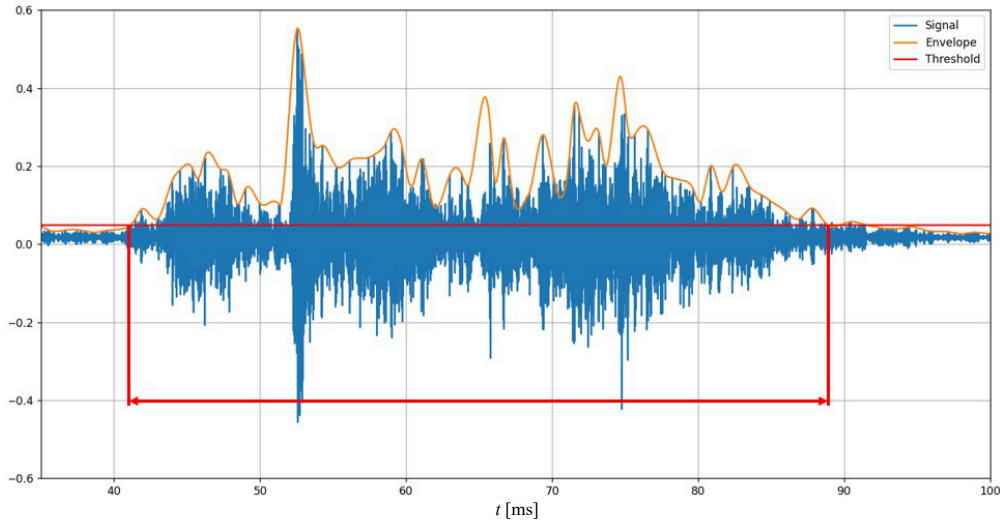


Fig. 7. AE signal generated by OLTC with plotted envelope. The switching time is determined as the time during which the envelope values are above the threshold.

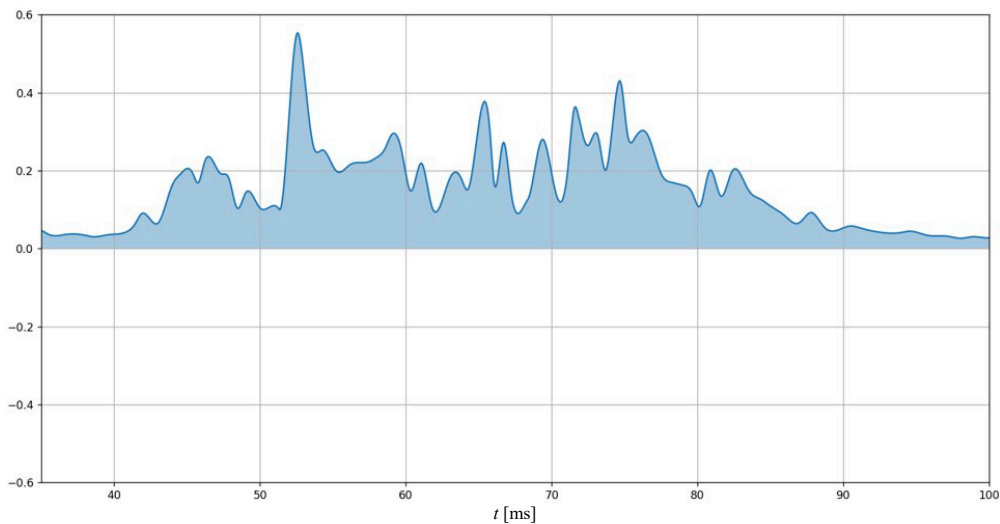


Fig. 8. Graphical representation of the descriptor describing the field under the acoustic emission signal envelope.

calculated for all cases. The second designated descriptor covers the area under the envelope, and a visualization of its determination is shown in Fig. 8.

All calculated descriptors and the relative differences between the values obtained for the symmetric and asymmetric systems are presented in Table 4. The switching duration increased significantly for the system with non-simultaneous operation, while the area under the envelope decreased. The time-frequency

analysis constituted the next stage in the analysis of the results. It was utilized not only to illustrate the differences in the frequency response of the different transducers but also to visualize the differences in frequencies found in systems with a defect relative to normal systems.

Figures 9–11 present the results of the time-frequency analysis of AE signals generated by OLTC with original and modified contacts. The presented

Table 4. Descriptors calculated in the time domain.

| | Transducer 1 | | | Transducer 2 | | | Transducer 3 | | |
|---------------------|--------------|-----------|-----------------------------|--------------|-----------|-----------------------------|--------------|-----------|-----------------------------|
| | Symmetry | Asymmetry | The relative difference [%] | Symmetry | Asymmetry | The relative difference [%] | Symmetry | Asymmetry | The relative difference [%] |
| Duration [ms] | 8.19 | 31.54 | 321.73 | 13.71 | 39.43 | 187.60 | 7.76 | 35.74 | 360.57 |
| Area under envelope | 4.14 | 2.6 | 37.20 | 4.49 | 2.93 | 34.74 | 2.83 | 2.13 | 24.73 |

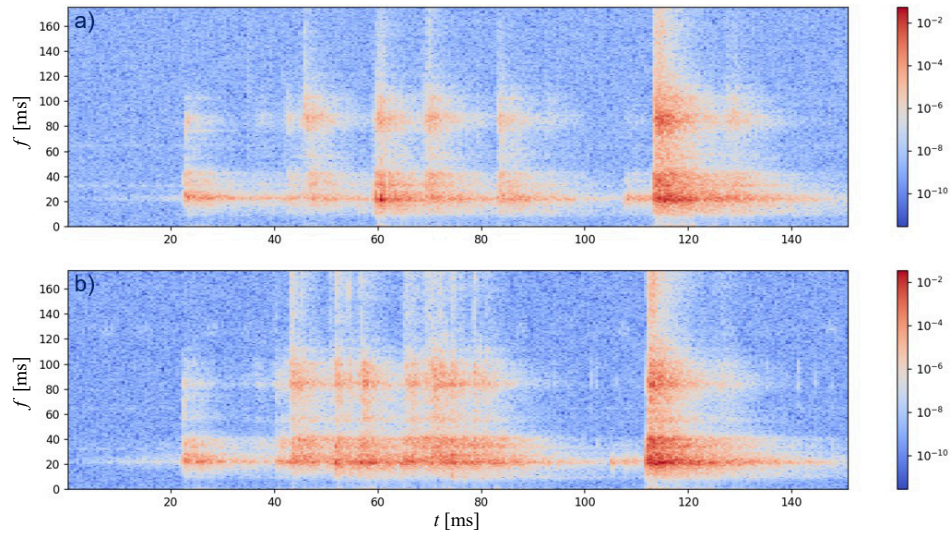


Fig. 9. Spectrogram of AE signal generated by OLTC recorded with transducer 1 for: a) system without asymmetry; b) system with asymmetry.

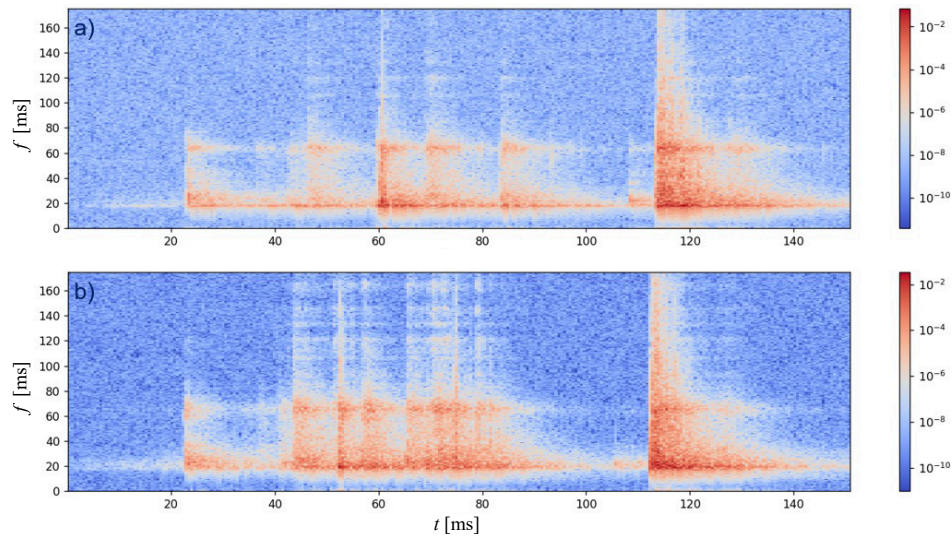


Fig. 10. Spectrogram of AE signal generated by OLTC recorded with transducer 2 for: a) system without asymmetry; b) system with asymmetry.

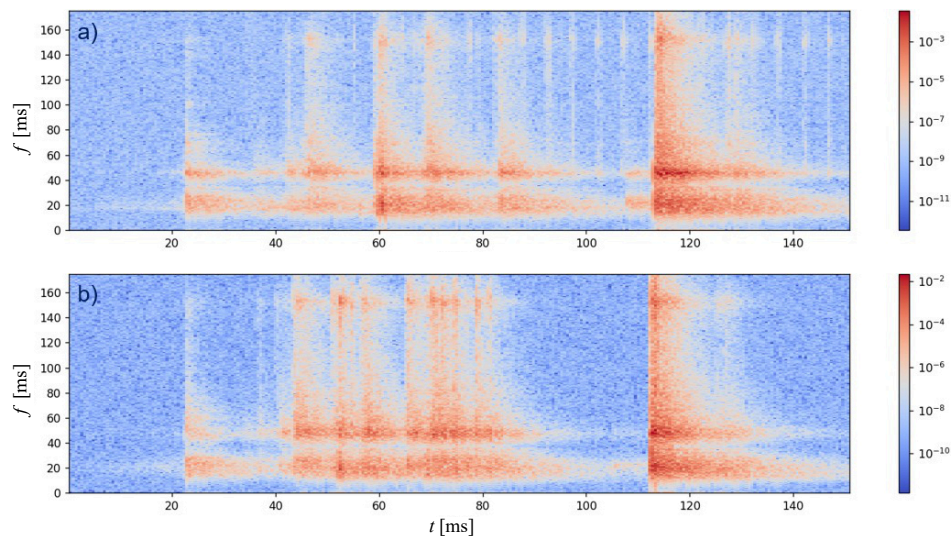


Fig. 11. Spectrogram of AE signal generated by OLTC recorded with transducer 3 for: a) system without asymmetry; b) system with asymmetry.

results cover the frequency band up to 175 kHz. This is due to the Nyquist frequency. Since OLTC tests are performed for mechanical damage, there is no need to analyze higher frequencies. For the modified system, the presence of a large number of acoustic events in the 40–90 ms range can be seen. These events correspond to individual switch strikes, occurring non-simultaneously for each phase.

In the case of an unmodified system, more discrete structures are visible and can be distinguished in time. In the case of the faulty device, an extension in time of the individual frequency structures is visible. They are relatively continuous in time, which makes it possible to identify a much larger number of unevenly occurring acoustic events resulting from unevenly switching contacts of the individual phases. In the case of uniform switching, we have a relatively synchronized switching cycle because the acoustic signals can be uniquely isolated from the recording. In the case of a modeled fault, this cannot be done. It should be noted that such a phenomenon is visible regardless of the type of transducer used. The clear differences observed in the spectrograms allow an unambiguous assessment of the presence of the defect under investigation.

Each of the transducers used allows the simultaneity of the switch to be assessed. However, the differences are most pronounced for transducer 3. For this transducer, the frequency structures describing the individual beats are most evident at higher frequencies;

thus, it is best suited when diagnosing OLTC using spectrograms of acoustic emission signals.

To avoid relying solely on visual analysis of the obtained waveforms and spectrograms during the diagnosis of OLTC, several descriptors were identified and used:

- maximum value (max);
- root mean squared (RMS);
- median;
- peak factor;
- form factor;
- frequency of highest amplitude.

These descriptors were applied in the analysis of amplitude and power density spectrum. For each of the descriptors analyzed, changes were observed after system modification. The results obtained make it possible to diagnose the switching asymmetry based on analytical data rather than visual inputs. The same procedure was performed on the power density spectrum. Values calculated for the amplitude spectrum are shown in Table 5, while in Table 6 values for the power density spectrum are presented.

The changes between the normal and modified systems are significant, confirming that it is possible to diagnose asymmetric performance based on the proposed descriptors. It can be seen that time series descriptors undergo the most significant changes. The system with asymmetric operation had a significantly

Table 5. Amplitude spectrum descriptors.

| | Transducer 1 | | | Transducer 2 | | | Transducer 3 | | |
|-------------|--------------|-----------|-----------------------------|--------------|-----------|-----------------------------|--------------|-----------|-----------------------------|
| | Symmetry | Asymmetry | The relative difference [%] | Symmetry | Asymmetry | The relative difference [%] | Symmetry | Asymmetry | The relative difference [%] |
| Max | 4.003E-06 | 5.435E-06 | 35.76 | 1.830E-05 | 8.889E-06 | 51.41 | 3.793E-06 | 1.248E-06 | 67.09 |
| RMS | 1.269E-07 | 1.583E-07 | 24.74 | 3.020E-07 | 1.961E-07 | 35.05 | 9.936E-08 | 5.535E-08 | 44.29 |
| Median | 3.594E-10 | 3.498E-10 | 2.66 | 2.129E-10 | 4.017E-10 | 88.70 | 5.661E-10 | 1.468E-09 | 159.40 |
| Peak factor | 3.154E+01 | 4.333E+00 | 86.26 | 6.059E+01 | 4.532E+01 | 25.19 | 3.817E+01 | 2.255E+01 | 40.92 |
| Form factor | 6.207E+00 | 6.421E+00 | 3.45 | 9.573E+00 | 6.459E+00 | 32.53 | 5.754E+00 | 3.744E+00 | 34.94 |
| F_{\max} | 21.00 kHz | 21.13 kHz | 0.60 | 17.86 kHz | 18.97 kHz | 6.17 | 45.53 kHz | 46.85 kHz | 2.90 |

Table 6. Power density spectrum descriptors.

| | Transducer 1 | | | Transducer 2 | | | Transducer 3 | | |
|-------------|--------------|-----------|-----------------------------|--------------|-----------|-----------------------------|--------------|-----------|-----------------------------|
| | Symmetry | Asymmetry | The relative difference [%] | Symmetry | Asymmetry | The relative difference [%] | Symmetry | Asymmetry | The relative difference [%] |
| Max | 1.927E+02 | 2.245E+02 | 16.52 | 4.119E+02 | 2.871E+02 | 30.30 | 1.876E+02 | 1.076E+02 | 42.63 |
| RMS | 1.377E+01 | 1.512E+01 | 9.80 | 1.710E+01 | 1.678E+01 | 1.89 | 1.266E+01 | 1.171E+01 | 7.47 |
| Median | 1.826E+00 | 1.801E+00 | 1.34 | 1.404E+00 | 1.930E+00 | 37.46 | 2.292E+00 | 3.690E+00 | 61.05 |
| Peak factor | 1.399E+01 | 1.485E+01 | 6.11 | 2.408E+01 | 1.711E+01 | 28.96 | 1.482E+01 | 9.187E+00 | 38.00 |
| Form factor | 2.279E+00 | 2.343E+00 | 2.84 | 2.562E+00 | 2.282E+00 | 10.92 | 2.118E+00 | 1.696E+00 | 19.91 |
| F_{\max} | 17.86 kHz | 18.97 kHz | 6.17 | 1.786E+04 | 1.897E+04 | 6.17 | 45.53 kHz | 46.85 kHz | 2.90 |

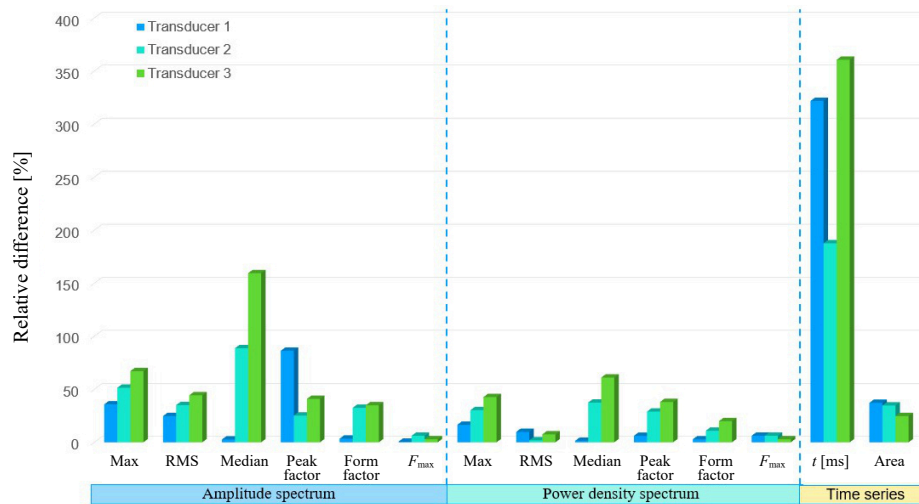


Fig. 12. Relative differences between normal and modified systems for each transducer.

longer switching duration than the normal system. The changes recorded in the descriptors determined based on the amplitude spectrum and power density are also significant.

In Fig. 12, all relative differences in values are plotted. By analyzing the graph, it is possible to determine the tested transmitters for the case yielding the best results in terms of diagnosing the studied defect.

4. Conclusion

On the basis of the analysis of the results obtained in the study, it was found that it is possible to diagnose non-simultaneous operation using each of the piezoelectric transducers subjected to testing. The differences are also clearly visible on the spectrograms. The differences between the time courses for the modified and unmodified systems are discernible, allowing the OLTC condition to be assessed through visual inspection. The assessment of the occurrence of non-simultaneous operations was simplified by calculating the descriptors given earlier. The differences in designated values are substantial, ranging up to 300%. This allows diagnosis to be carried out even by staff members who do not have specialized knowledge. In addition, the ability to carry out OLTC diagnostics without the need to shut down the transformer offers more frequent measurements to be carried out. It is also possible to use the AE method for continuous measurements. The results demonstrate that transducers with different characteristics can be used for AE diagnostics. This opens up the possibility of using transducers to detect partial discharges to monitor the mechanical state of the OLTC.

By comparing relative differences between individual descriptors, we are able to identify the transducer that can be the most useful for diagnosing non-simultaneous operation. The number of descriptors for

which the transducer achieved the highest relative difference value:

- transducer 1: 4 differences;
- transducer 2: 2 differences;
- transducer 3: 9 differences.

For transducer 3, the highest number of differences was registered. Therefore, it was concluded that it is the most suitable one for diagnostic purposes.

Two new descriptors, calculated from time series, were introduced, one to describe the duration of the switching event and the other to establish the field under the envelope. These have proven valuable in assessing the symmetry of OLTC operations. Thus, their use in developing an expert system for OLTC diagnostics will allow more efficient identification of the defect under investigation.

The results presented in this paper indicate differences in the AE signals generated by normal system and asymmetrically switching systems. The significant advantage of the AE diagnostic method is to perform diagnosis in a non-destructive way, as it is not necessary to take the unit out of service. Correct interpretation of time courses can be quite a challenging task, so future work will focus on evaluating the potential for detecting different kinds of damages using artificial intelligence.

The research presented in the paper forms one of the phases of work aimed at creating an expert system for online diagnosis of OLTC. The descriptors analyzed in this paper have demonstrated their feasibility in diagnosing non-simultaneity and will, therefore, be used as one of the input parameters for neural network. For other defects, a similar analysis will be carried out. This will allow the creation of a set of descriptors that fully describe the performance of OLTC. Further work will also focus on examining the possibility of using the presented method to determine the technical condition of other types of OLTC. It is expected that after

determining the values of the described descriptors for undamaged OLTCs of other types, they will be successfully used as a reference point for determining defects occurring in the described devices.

References

1. AZIZ M.A.A., TALIB M.A., ARUMUGAM R. (2014), Diagnosis of on-load tap changer (OLTC) using dynamic resistance measurement, [in:] *IEEE 8th International Power Engineering and Optimization Conference (PEOCO2014)*, pp. 494–497, doi: [10.1109/PEOCO.2014.6814479](https://doi.org/10.1109/PEOCO.2014.6814479).
2. BORICIC A. *et al.* (2019), Dynamic resistance measurements and result interpretation for various on-load tap changers, [in:] *IEEE Milan PowerTech*, pp. 1–6, doi: [10.1109/PTC.2019.8810530](https://doi.org/10.1109/PTC.2019.8810530).
3. CICHÓN A., BORUCKI S., BOCZAR T. (2011a), Diagnosis of the non-concurrent operation of the on-load tap changer contacts by the acoustic emission method, *Archives of Acoustics*, **36**(4): 823–830, doi: [10.2478/v10168-011-0054-4](https://doi.org/10.2478/v10168-011-0054-4).
4. CICHÓN A., BORUCKI T., BOCZAR T., ZMARZLY D. (2011b), Characteristic of acoustic emission signals generated by electric arc in on load tap changer, [in:] *Proceedings of 2011 International Symposium on Electrical Insulating Materials*, pp. 437–439, doi: [10.1109/ISEIM.2011.6826306](https://doi.org/10.1109/ISEIM.2011.6826306).
5. CICHÓN A., BORUCKI T., BOCZAR T., ZMARZLY D. (2012), The possibilities of using acoustic signals generated by the on load tap changer, [in:] *Proceedings of the 41st International Congress and Exposition on Noise Control Engineering 2012*.
6. DUAN R., WANG F. (2015), Mechanical condition monitoring of on-load tap-changers using chaos theory & fuzzy C-means algorithm, [in:] *IEEE Power and Energy Society General Meeting*, doi: [10.1109/PESGM.2015.7286077](https://doi.org/10.1109/PESGM.2015.7286077).
7. Energo-Complex (2008), MT-3 v.3 Technical description, <https://energo-complex.pl/wp-content/uploads/2018/03/ENERGO-COMPLEX-Przyrzad-do-badania-transformatorow-MT-3.pdf> (access: 02.04.2023).
8. JONGEN R., GULSKI E., SIODŁA K., PARCIAK J., ERBRINK J. (2014), Diagnosis of degradation effects of on-load tap changer in power transformers, [in:] *ICHVE International Conference on High Voltage Engineering and Application*, doi: [10.1109/ICHVE.2014.7035469](https://doi.org/10.1109/ICHVE.2014.7035469).
9. JONGEN R., SEITZ P.P., SMIT J., STREHL T., LEICH R., GULSKI E. (2012), On-load tap changer diagnosis with dynamic resistance measurements, [in:] *IEEE International Conference on Condition Monitoring and Diagnosis*, pp. 485–488, doi: [10.1109/CMD.2012.6416184](https://doi.org/10.1109/CMD.2012.6416184).
10. KANG P., BIRTHWHISTLE D. (2001a), Condition monitoring of power transformer on-load-tap-changers. Part 1: Automatic condition diagnostics, *IEE Proceedings – Generation, Transmission and Distribution*, **148**(4): 301–306, doi: [10.1049/ip-gtd:20010389](https://doi.org/10.1049/ip-gtd:20010389).
11. KANG P., BIRTHWHISTLE D. (2001b), Condition monitoring of power transformer on-load-tap-changers. Part 2: Detection and aging from vibration signature, *IEE Proceedings – Generation, Transmission and Distribution*, **148**(4): 307–311, doi: [10.1049/ip-gtd:20010388](https://doi.org/10.1049/ip-gtd:20010388).
12. LI Q., ZHAO T., ZHANG L., LOU J. (2012), Mechanical fault diagnostics of on-load tap changer within power transformers based on hidden Markov model, [in:] *IEEE Transactions on Power Delivery*, **27**(2): 596–601, doi: [10.1109/TPWRD.2011.2175454](https://doi.org/10.1109/TPWRD.2011.2175454).
13. MAJCHRZAK H., CICHÓN A., BORUCKI S. (2016), Application of the acoustic emission method for diagnosis in on-load tap changer, *Archives of Acoustics*, **42**(1): 29–35, doi: [10.1515/aoa-2017-0004](https://doi.org/10.1515/aoa-2017-0004).
14. MISTRAS Group (n.d.a), WD Sensor, Product brochure, https://www.physicalacoustics.com/content/literature/sensors/Model_WD.pdf (access: 02.04.2023).
15. MISTRAS Group (n.d.b), D9241A Sensor, Product brochure, <https://pdf.directindustry.com/pdf/physical-acoustics/d9241a-sensor/27111-396871.html> (access: 02.04.2023).
16. MISTRAS Group (n.d.c), R15 α Sensor, Product brochure, <https://pdf.directindustry.com/pdf/physical-acoustics/r15-alpha/27111-396891.html> (access: 02.04.2023).
17. OSMANBASIC E., SKELO G. (2017), Tap changer condition assessment using dynamic resistance measurement, *Procedia Engineering*, **202**: 52–64, doi: [10.1016/j.proeng.2017.09.694](https://doi.org/10.1016/j.proeng.2017.09.694).
18. SCHELLHASE H.-U., POLLOCK R.G., RAO A.S., KOROLENKO E.C., WARD B. (2002), Load tap changers: Investigations of contacts, contact wear and contact coking, [in:] *Proceedings of the Forty-Eighth IEEE Holm Conference on Electrical Contacts*, pp. 259–272, doi: [10.1109/HOLM.2002.1040850](https://doi.org/10.1109/HOLM.2002.1040850).
19. SECIC A., KUZLE I. (2017), On the novel approach to the on load tap changer (OLTC) diagnostics based on the observation of fractal properties of recorded vibration fingerprints, [in:] *IEEE EUROCON 2017 – 17th International Conference on Smart Technologies*, pp. 720–725, doi: [10.1109/EUROCON.2017.8011205](https://doi.org/10.1109/EUROCON.2017.8011205).
20. SEO J., MA H., SAHA T.K. (2017), A joint vibration and arcing measurement system for online condition monitoring of on-load tap changer of the power transformer, [in:] *IEEE Transactions on Power Delivery*, **32**(2): 1031–1038, doi: [10.1109/TPWRD.2016.2531186](https://doi.org/10.1109/TPWRD.2016.2531186).
21. WOTZKA D., CICHÓN A. (2020), Study on the influence of measuring AE sensor type on the effectiveness of OLTC defect classification, *Sensors*, **20**(11): 3095, doi: [10.3390/s20113095](https://doi.org/10.3390/s20113095).
22. WOTZKA D., CICHÓN A., MANOWSKI P. (2019), Classification of OLTC defects based on AE signals measured by two different transducers, *20th International Scientific Conference on Electric Power Engineering (EPE)*, pp. 1–5, doi: [10.1109/EPE.2019.8778140](https://doi.org/10.1109/EPE.2019.8778140).